

Design of Common-Source/Drain Active Balun Using 90nm CMOS Technology

Frederick Ray I. Gomez^{1,2*}, Maria Theresa G. De Leon¹,
John Richard E. Hizon¹

¹University of the Philippines, Diliman, Quezon City, Philippines 1101
²STMicroelectronics, Inc., Calamba City, Laguna, Philippines 4027

ABSTRACT

This research paper presents a design and study of a common-source/drain active balun circuit implemented in a standard 90-nm complementary metal-oxide semiconductor (CMOS) technology. The active balun design is intended for worldwide interoperability for microwave access (WiMAX) application, with operating frequency of 5.8GHz and supply voltage of 1V. Measurements are taken for parameters namely gain difference, phase difference, and noise figure. The common-source active balun design achieved a minimal gain difference of 0.016dB, phase difference of $180^\circ \pm 7.1^\circ$, and noise figure of 7.42-9.85dB, which are comparable to past active balun designs and researches. The design eventually achieved a low power consumption of 2.56mW.

Keywords: Common-source/drain active balun; 90nm CMOS; balun; gain; gain difference, phase difference, noise figure; WiMAX

1. INTRODUCTION

A considerable growth of interest in technologies that could deliver higher data rates over wider coverage led to the evolution of new wireless standards such as the IEEE 802.16-based WiMAX or the worldwide interoperability for microwave access. Like WiMAX, other communication systems namely Bluetooth, Wireless Fidelity (WiFi), and Long-Term Evolution (LTE) have the radio frequency (RF) receiver front-end that proves to be a critical part in the wireless system. A typical wireless receiver is represented in Fig. 1 diagram.

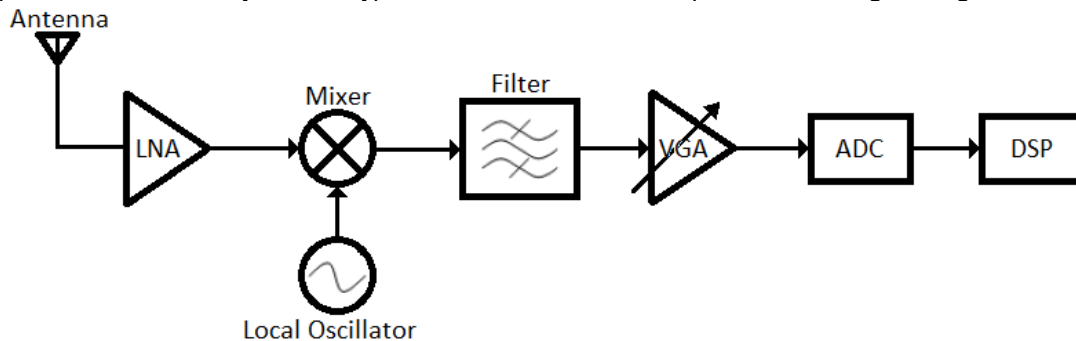
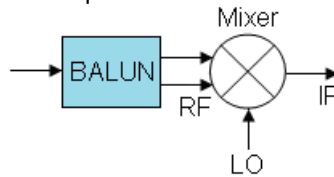


Fig. 1. Block diagram of a wireless receiver

32 Some of RF front-end circuits are often designed as differential circuits. Fully-differential
33 approach is usually preferred in RFIC design due to its advantages, particularly the high
34 immunity to common-mode noises, rejection to parasitic couplings, and increased dynamic
35 range [1-2]. In order to supply input signal to differential circuits, a building block capable of
36 supplying balanced differential signals is needed without sacrificing the performance of the
37 overall system in terms of gain, noise figure, and linearity. Active balun (balanced-
38 unbalanced) is capable to perform the necessary tasks.
39

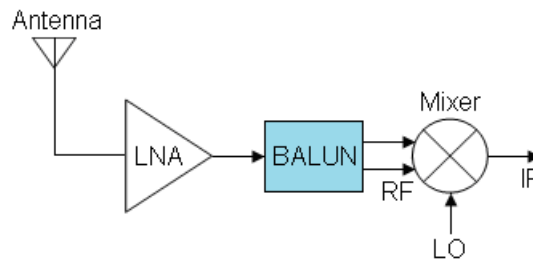
40 A balun circuit is a type of transformer that converts signals that are single-ended or
41 unbalanced with respect to ground into signals that are differential or balanced with respect
42 to ground, and vice versa. Baluns can be classified as either active or passive baluns
43 depending on the devices used. Active baluns, although unidirectional and more complex to
44 implement, are preferred over their passive counterparts because they can produce gain,
45 occupy less chip area and can operate at higher frequencies [2-3].
46

47 Active balun circuit can be used as the first block of the WiMAX receiver front-end to supply
48 differential signal to a differential low-noise amplifier (LNA) [4]. It can also be used to supply
49 differential signal to a mixer [5] in Fig. 2. Fig. 3 illustrates the active balun circuit as an
50 intermediate block between the LNA and the mixer [6]. Note that the configuration depends
51 on the gain, noise figure (NF), and linearity requirements of the system. Since LNA is the
52 first block in the receiver front end, it is critically designed with high gain of at least 25dB and
53 noise figure of less than 2dB. Based on past researches, active balun has relatively high
54 noise figure and lower gain performance compared to LNA, hence cannot be considered as
55 the first block in the receiver front-end. Finally, the challenge is to design an active balun as
56 an intermediate block to allow the LNA's output to connect with a differential mixer's input,
57 with performance conforming to the requirement for the WiMAX receiver front-end.



58
59
60
61

Fig. 2. Active balun supplying a differential mixer



62
63
64
65
66

Fig. 3. Active balun as intermediate block between LNA and mixer

67 2. ACTIVE BALUN DESIGN

68
69 In this research paper, a common-source/drain active balun is designed and implemented in
70 a standard 90nm complementary metal-oxide semiconductor (CMOS) technology. Process
71 design kit (PDK) for standard 90nm CMOS process from CMP (Circuits Multi Projets) and

72 **STMicroelectronics was used for the design.** The supply voltage (V_{DD}) for the design is set to
 73 1V. The lengths (L) of all transistors are set to 100nm, which is the minimum allowed
 74 channel length for the technology used. Transistor widths (W) are carefully computed to
 75 ensure the operation of all the transistors at saturation. As mentioned earlier, the paper
 76 deals with the design of active baluns as intermediate block between LNA and mixer in the
 77 WiMAX receiver front-end. Table 1 summarizes the target specifications of the active balun
 78 design. These values are based from past active balun researches [5-8] and from the
 79 summary of parameters as per WiMAX standard [9].
 80
 81

Table 1. Target specifications for the common-source/drain active balun design

Parameters	Value
Frequency	5.8GHz
Gain difference	< 1dB
Phase difference	$180^\circ \pm 10^\circ$
Noise figure	< 10dB
Power consumption	< 10mW

82
 83 Two important parameters of the active balun are the gain difference and phase difference.
 84 Gain difference is the difference of the gains from the two output nodes of the active balun
 85 while the phase difference is the difference between the phase of the non-inverting output
 86 node (RFout1) and the phase of inverting output node (RFout2) of the active balun. Another
 87 important parameter is the noise figure (NF), which is the measure of the amount signal-to-
 88 noise-ratio (SNR) degradation introduced by the circuit as seen in the output.
 89

90 The common-source/drain active balun shown in Fig. 4 is composed of a single transistor
 91 M1. The input signal is fed into the gate of the transistor. Normal operation results in an
 92 inverted output signal at RFout2 and a non-inverted signal at RFout1. Ideally, these two
 93 outputs would have the same amplitude with a phase difference of 180° . Load resistors R1
 94 and R2 determine the output voltages as well as the voltage gains of the two output signals
 95 with respect to the input signal.

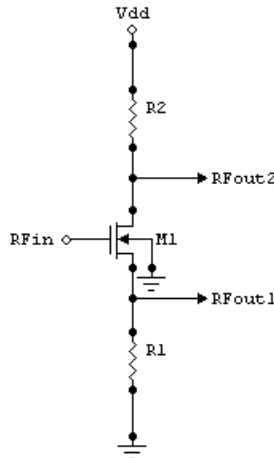


Fig. 4. Common-source/drain active balun schematic

96
 97
 98
 99
 100 Common-source topology exhibits a relatively high input impedance while providing voltage
 101 gain and requiring a minimal voltage headroom. Common-drain topology or source-follower,
 102 on the other hand, is sometimes employed as level shifters or buffers, impacting the overall

103 frequency response. It also exhibits high input impedance. With the two topologies merged
 104 to function as an active balun, common-drain will dominate the response on the overall
 105 voltage gain or attenuation because of the feedback effect of load resistor R1 with respect to
 106 the input.

107
 108 Common-source/drain active balun is ideal for low voltage, low power WiMAX application
 109 due to low number of stacked devices. The active balun cannot actually produce gain in
 110 RFout1 due to its source-follower configuration. Since the two outputs should have
 111 balanced gain or attenuation, RFout2 should adjust and thus cannot produce gain. Hence,
 112 one important goal for this active balun design is to minimize the attenuation in outputs
 113 RFout1 and RFout2 and should be balanced with respect to the input RFin.

114
 115 Drain current I_{DS} of transistor M1 is also the total supply current that is derived from the total
 116 power consumption of the active balun. With supply voltage $V_{DD} = 1V$, I_{DS} could be
 117 computed in Eq. (1) in terms of the output DC or bias voltages V_1 (or V_{RFout1}) and V_2 (or
 118 V_{RFout1}) and the output loads R1 and R2.

$$I_{DS} = \frac{V_1 - 0}{R1} = \frac{V_{DD} - V_2}{R2} \rightarrow I_{DS} = \frac{V_1}{R1} = \frac{1V - V_2}{R2} \quad \text{Eq. (1)}$$

120 Assuming output loads R1 and R2 are equal to achieve a balanced response for V_1 and V_2
 121 in terms of output swing, Eq. (1) would become Eq. (2).

$$V_1 = 1V - V_2 \quad \text{Eq. (2)}$$

122
 123 From the expression in Eq. (1), increasing I_{DS} increases the output voltage V_1 , while output
 124 voltage V_2 decreases with I_{DS} . To achieve the minimum attenuation, V_1 and V_2 should take
 125 into account the drain-to-source voltage V_{DS} of transistor M1. This will also maximize the
 126 output swing in RFout1 and RFout2. Ensuring that transistor M1 operates at saturation
 127 region, V_{DS} should be at least V_{DSAT} or the overdrive voltage V_{OV} . With supply voltage $V_{DD} =$
 128 $1V$, overdrive voltage V_{OV} set to 200mV and with the two outputs balanced, output voltage
 129 swings are computed as

$$V_{DS} = V_2 - V_1 \geq V_{DSAT} \rightarrow V_2 - V_1 \geq 0.2V \quad \text{Eq. (3)}$$

131 Substituting V_1 expression in Eq. (2) into Eq. (3),

$$V_2 - (1V - V_2) \geq 0.2V \quad \text{Eq. (4)}$$

$$V_2 \geq 0.6V \rightarrow 1V > V_2 \geq 0.6V \quad \text{Eq. (5)}$$

132
 133 Output DC voltage V_2 is computed to swing from 0.6V to 1V. Calculating for the output
 134 swing for V_1 ,

$$V_2 - V_1 = V_{DS,Q} \geq 0.2V \rightarrow V_1 \leq V_2 - 0.2V \quad \text{Eq. (6)}$$

$$V_1 \leq 0.6V - 0.2V \quad \text{Eq. (7)}$$

$$V_1 \leq 0.4V \rightarrow 0.4V \geq V_1 > 0 \quad \text{Eq. (8)}$$

135
 136 Output DC voltage swing for V_1 is calculated to range from 0V to 0.4V. As previously
 137 mentioned, V_1 increases with I_{DS} while V_2 decreases with I_{DS} . To maximize the output
 138 swing in RFout1 and RFout2, output DC voltages V_1 and V_2 should have values median to
 139 their output range in Eq. (8) and Eq. (5), respectively. This would also safeguard transistor

140 M1 to operate at saturation region with V_{DS} of at least 200mV, while varying I_{DS} . The
 141 optimized values for output DC voltages V_1 and V_2 are given as

$$V_1 = 0.2V \quad \text{Eq. (9)}$$

$$V_2 = 0.8V \quad \text{Eq. (10)}$$

142 With threshold voltage V_t set to 400mV, V_{OV} set to 200mV, V_1 set to 0.2V, and $V_{DS} \geq V_{DSAT} =$
 143 V_{OV} , input bias voltage could be determined in Eq. (11) to (12).
 144

$$V_{DS} = V_{GS} - V_t \geq V_{DSAT} \quad \rightarrow \quad (V_{IN} - 0.2V) - 0.4V = 0.2V \quad \text{Eq. (11)}$$

$$V_{IN} = 0.8V \quad \text{Eq. (12)}$$

145 With input DC voltage V_{IN} set to 0.8V, it could swing from maximum 1V to 0.6V. Maximum
 146 input voltage is set to align with the supply voltage V_{DD} which is at 1V. Drain current I_{DS} of
 147 transistor M1 is also the total current that is derived from the total power consumption of the
 148 active balun. Using the square-law equation in Eq. (13), transconductance g_m could be
 149 computed in Eq. (14) to (15).
 150

$$I_D = \frac{\mu C_{ox} W}{2 L} (V_{GS} - V_t)^2 (1 + \lambda V_{DS}) \quad \text{Eq. (13)}$$

$$g_m = \frac{\delta I_{DS}}{\delta V_{GS}} = \mu C_{ox} \frac{W}{L} (V_{GS} - V_t) (1 + \lambda V_{DS}) \quad \text{Eq. (14)}$$

$$g_m = \mu C_{ox} \frac{W}{L} (V_{IN} - V_t - V_1) (1 + \lambda V_{DS}) \quad \text{Eq. (15)}$$

151 Substituting I_{DS} from Eq. (13) into g_m in Eq. (14), an important design parameter could be
 152 determined, which is the gmoverld.
 153

$$g_m = \frac{\delta I_{DS}}{\delta V_{GS}} = \frac{2I_{DS}}{(V_{GS} - V_t)} = \frac{2I_{DS}}{V_{OV}} = \frac{2I_{DS}}{V^*} = \frac{2I_{DS}}{(V_{IN} - V_1 - V_t)} \quad \text{Eq. (16)}$$

$$\frac{g_m}{I_{DS}} = gmoverld = \frac{2}{(V_{IN} - V_t - I_{DS}R_1)} \quad \text{Eq. (17)}$$

154 Proper DC input bias should be observed to realize good efficiency in terms of gmoverld. It
 155 can also be observed that the gmoverld is affected by the load resistance R1. For low power
 156 design, higher gmoverld is recommended [10]. As initially assumed, V_{OV} is set 200mV for
 157 minimum attenuation and/or maximum voltage swing in outputs R_{Fout1} and R_{Fout2} with
 158 respect to the input R_{Fin}. With this, gmoverld could be estimated in Eq. (18).
 159

$$\frac{g_m}{I_{DS}} = \frac{2}{200mV} = 10V^{-1} \quad \text{Eq. (18)}$$

160 It can be noted that to maintain the efficiency for low power consumption, lowering I_{DS} would
 161 also mean lowering g_m . Transistor sizing depends on the target power consumption and
 162 likewise I_{DS} , thus, affecting g_m . Transconductance g_m is a key parameter that determines the
 163 voltage gain of the active balun, which will be discussed in the succeeding section.
 164

165 Resistors R1 and R2 could be determined given the setup for minimum attenuation and
 166 maximum voltage swing in the two outputs.
 167

$$R1 = \frac{V_1}{I_{DS}} = \frac{0.2V}{I_{DS}} \quad R2 = \frac{V_{DD} - V_2}{I_{DS}} = \frac{0.2V}{I_{DS}} \quad \text{Eq. (19)}$$

168
169
170
171
172
173
174
175
176
177
178
179
180
181
182

To have a balanced attenuation in the two outputs, R1 should be equal to R2. With V_1 and V_2 set to the optimum value and V_{DD} set to 1V, decreasing the supply current (which is equal to I_{DS}) would increase the value of R1 and R2. Large resistor values contribute to more noise and parasitics. Since the active balun is targeted for low power consumption, tradeoff between drain current I_{DS} and resistor values is inevitable. Moreover, the design is optimized to meet the target performance specifications suitable for WIMAX receiver. The active balun was designed using Cadence Virtuoso software [11], a computer-aided design (CAD) tool and simulation software. The Composer Schematic program of the same software [11] is used for the transistor-level design, with the 90nm CMOS technology PDK. Moreover, Analog Artist tool of Cadence [11] was used for the simulation. Table 2 summarizes the common-source/drain active balun parameters.

Table 2. Common-source/drain active balun parameters expressions

Parameters	Value
Input bias voltage	0.8V
Output DC voltage for maximum swing	0.2V (RFout1), 0.8V (RFout2)
Input impedance	∞
Output impedance, with resistor and capacitor loads	$R1 \parallel 1/sC1$ (RFout1), $R2 \parallel 1/sC2$ (RFout2)
Voltage gain, simplified ($s = 0$)	$\frac{g_m R1}{1 + (g_m + g_{mb})R1}$ (RFout1) $\frac{-g_m R2}{1 + (g_m + g_{mb})R1}$ (RFout2)
Output noise voltage	$\frac{k_B T}{C1} [1 + \gamma(g_m + g_{mb})R1]$ (RFout1) $\frac{k_B T}{C2} [1 + \gamma(g_m + g_{mb})R2]$ (RFout2)
Noise Figure	$10 \log \left[1 + \frac{1 + \gamma(g_m + g_{mb})R1}{C1 \cdot k_B T \Delta f \cdot A_{v1}} \right]$ (RFout1) $10 \log \left[1 + \frac{1 + \gamma(g_m + g_{mb})R2}{C2 \cdot k_B T \Delta f \cdot A_{v2}} \right]$ (RFout2)

183
184

185 **3. RESULTS AND DISCUSSION**

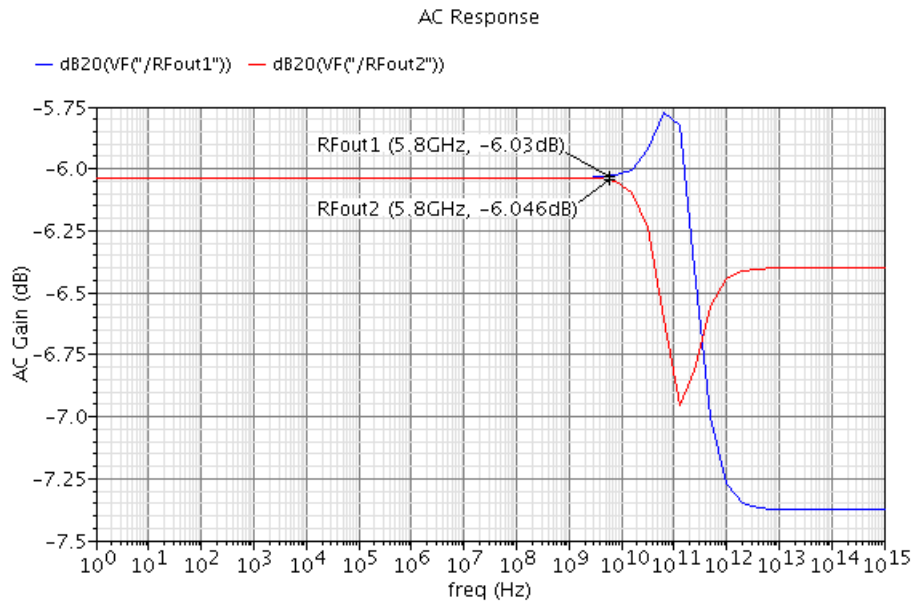
186

187 The common-source/drain active balun is characterized and designed to achieve the target
188 specifications. The extraction of all device parameters for use in simulations is done using
189 Synopsys Star-RCXT [12]. Simulations of the extracted view are done using Cadence
190 Design Systems software. The active balun is designed to operate at 5.8GHz, which is a
191 typical frequency for WiMAX applications. Measurements in the simulation plots are taken at
192 5.8GHz.
193

194 **3.1 Gain and Gain Difference**

195

196 There are many types of power gain defined for an amplifier. The most commonly specified
197 and often the most useful is the transducer gain, G_T . It is defined as the ratio of the power
198 delivered to the load to the power available from the source. Gain difference or gain error is
199 the difference of the gains from the two output nodes of the active balun, and is considered
200 as one of the most important parameters of the active balun design. Ideally, the gain
201 difference of an active balun should be zero in magnitude. The responses in Fig. 5 and Fig.
202 6 for the gain and gain difference, respectively, are determined using AC analysis. Ideal
203 voltage source is used with input bias voltage V_{IN} set to 0.8V. Drain-to-source voltage, $V_{DS,Q}$
204 = $V_2 - V_1$, was measured at 528.6mV with $V_{GS} - V_t = 71.6mV$, confirming the transistor M1
205 operating at saturation. Fig. 5 shows the response using AC analysis.



206

207

208

209

Fig. 5. AC analysis, gain plot

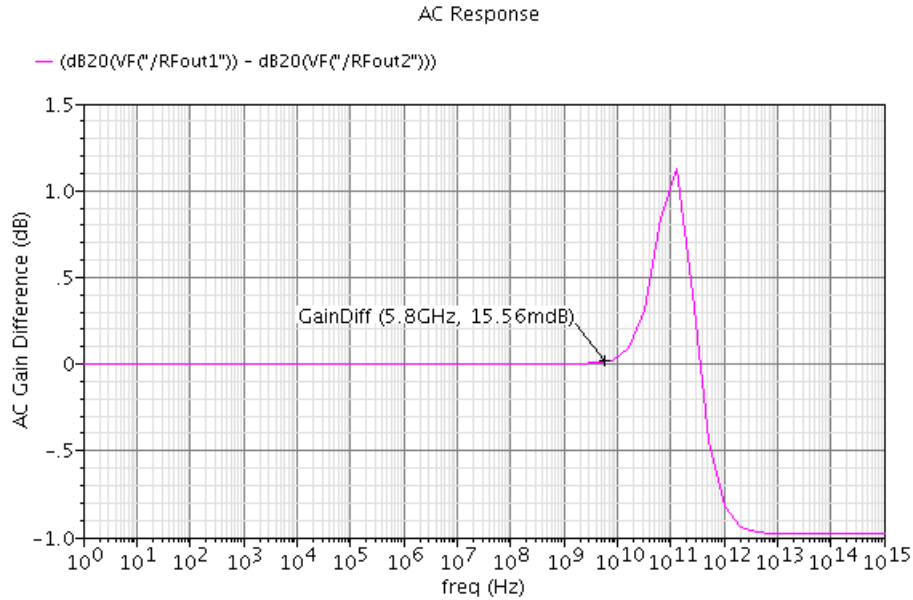


Fig. 6. AC analysis, gain difference plot

210
211
212
213
214
215
216
217
218
219

Since the active balun has the configuration of common-drain, it is expected that the gains would fall below the target of at least 0dB. AC gains are at around -6dB. Take note that the three active baluns are designed with ideal voltage source at the input, thus with very high (if not infinite) input impedance, and the output is left with no termination. Since the resistor loads of the active balun are of the same value, gain difference was maintained very low at 0.015dB.

220

3.2 Phase and Phase Difference

221

222

223

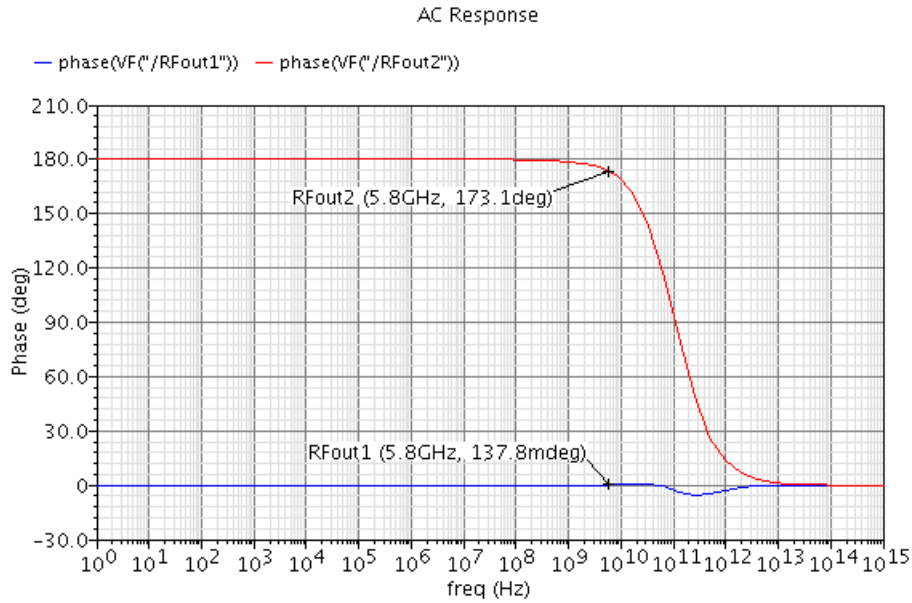
224

225

226

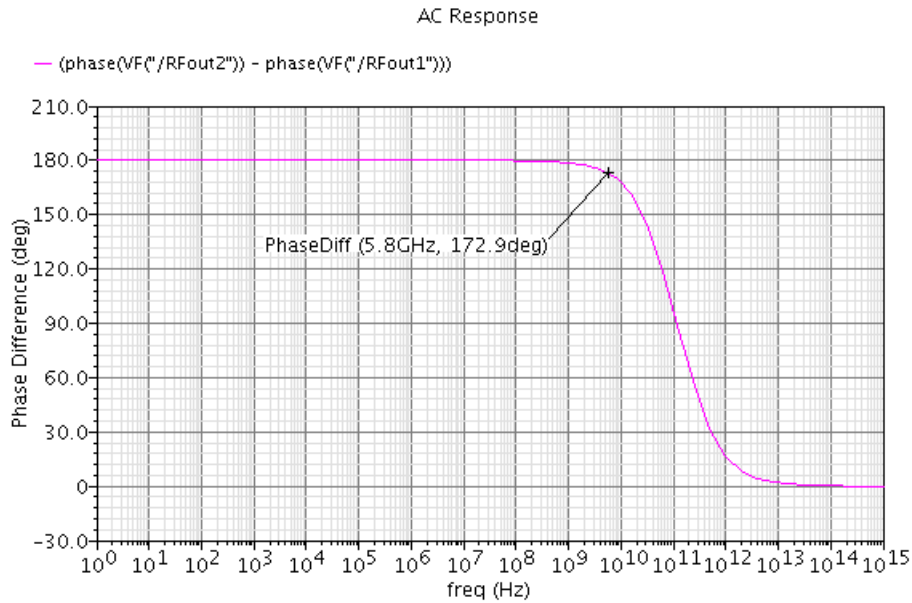
Another important parameter of an active balun is the phase difference. Phase difference is the difference between the phase of the non-inverting output node and the phase of inverting output node of the active balun. Figs. 7 and 8 show the AC analysis phase and phase difference responses, with ideal input voltage source.

227



228
229
230

Fig. 7. AC analysis, phase plot



231
232
233

Fig. 8. AC analysis, phase difference plot

234 Same analysis with the gain and gain difference are done with the phase and phase
235 difference. The results are within the acceptable values especially for the target phase
236 difference with measurement at 172.9°.

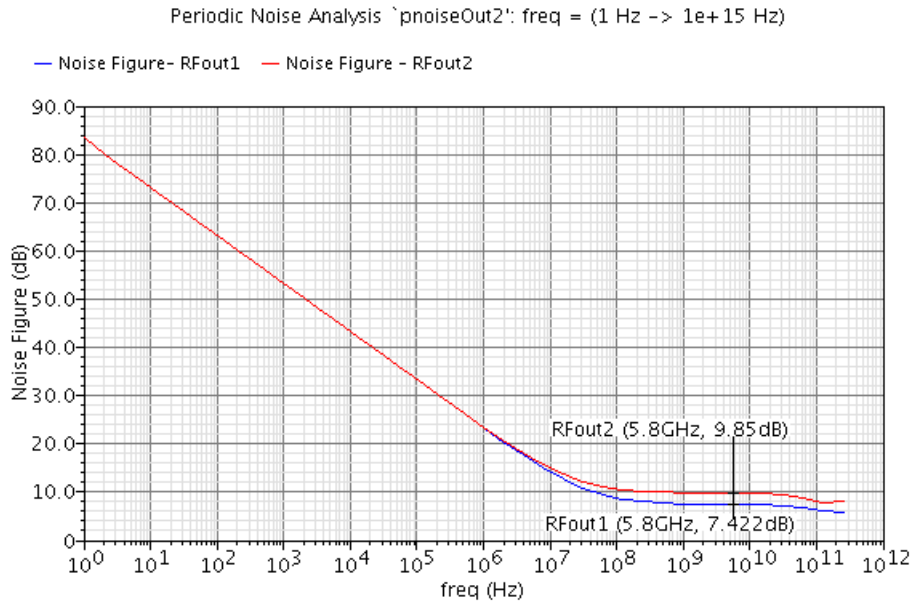
237

238 3.3 Noise Figure

239

240 Noise performance is an important design consideration since it determines the susceptibility
241 of the active balun to unwanted signal or noise. One important design parameters is the

242 noise figure (NF), which is a measure of the amount of signal-to-noise-ratio degradation
 243 introduced by the circuit as seen at the output. Fig. 9 shows the noise figure result using
 244 **periodic steady-state + periodic noise (PSS+PNoise)** analysis.
 245



246 **Fig. 9. Noise figure plot**

247
 248
 249 Noise figure of 7.422dB and 9.85dB for RfOut1 and RfOut2 with respect to RFin are
 250 generated using PSS+PNoise analysis with RF input power set to -20dBm. It is worth noting
 251 that the noise figure from PNoise analysis is slightly higher than the noise figure generated
 252 from SP analysis because at prf = -20dBm the active balun demonstrated very weak
 253 nonlinearity and noise as other high harmonics are convoluted.
 254

255 **3.4 Results Summary**

256
 257 Table 3 summarizes the performance of **the common-source/drain active balun design, and**
 258 **comparison with past active balun designs and researches.**
 259

260 **Table 3. Performance summary of **common-source/drain active balun****

261

Parameters	Target Specs	Common-Source/Drain Active Balun Design	[5]	[7]
Topology		Common-Source/Drain	Common-Source with Common-Gate	Differential
Process/Technology	90nm CMOS	90nm CMOS	0.18µm CMOS	0.18µm CMOS
Supply voltage	1V	1V	1.2V	1.5V
Frequency	5.8GHz	5.8GHz	~8GHz	5.1~5.9GHz
Gain difference	< 1dB	0.016dB	2dB	0.020dB
Phase	180° ± 10°	172.9°	183°	180.58°

difference				
Noise figure	< 10dB	7.422dB (RFout1), 9.850dB (RFout2)	11dB	--
Power consumption	< 10mW	2.558mW	1.44mW	9.17mW

262
263 The common-source/drain active balun design achieved a gain difference better than 1dB
264 and a phase difference of $180^{\circ} \pm 10^{\circ}$ or better at frequency of 5.8GHz. The balun is affected
265 with the input and output loading since the circuit is designed with ideal input voltage source
266 and no termination ports included. Low power consumption of at most 2.56mW is achieved,
267 comparable to other low power designs in the past researches.

268
269

270 **4. CONCLUSION AND RECOMMENDATIONS**

271

272 A common-source/drain active balun is designed and implemented in a standard 90nm
273 CMOS process, and carefully designed to satisfy the WiMAX receiver requirement at
274 5.8GHz. Simulation measurements are taken for parameters such as gain, phase, gain
275 difference, phase difference, and noise figure.

276 The design achieved gain difference of less than 0.02dB and phase difference of $180^{\circ} \pm$
277 7.1° . Noise figure performance is at around 7.42–9.85dB, comparable to previous designs
278 and researches. Low power consumption of at most 2.56mW is achieved, comparable to
279 other low power designs.

280 Future work could include designing active balun with high gain. Although it will sacrifice the
281 bandwidth, it can still be realized at lower frequencies for practical applications. One
282 possible work would be to integrate the active balun functionality on the circuit design of a
283 differential circuit like that of the double-balanced mixer or differential LNA.

284
285

286 **ACKNOWLEDGMENTS**

287

288 The authors would like to express sincere gratitude to the Department of Science and
289 Technology (DOST), the Philippine Council for Advanced Science and Technology Research
290 and Development under DOST (DOST-PCASTRD), and the Engineering Research and
291 Development for Technology Consortium (DOST-ERDT) for the extensive support. The
292 authors would also like to thank the Microelectronics and Microprocessors Laboratory team
293 of the University of the Philippines for the technical support during the course of the study.
294 Author F.R. Gomez is greatly thankful to the STMicroelectronics Calamba Central
295 Engineering and Development Team and the Management Team for the utmost support.

296
297

298 **REFERENCES**

299

- 300 1. Crols J, Donnay S, Steyaert M, Gielen G. A high-level design and optimization tool for
301 analog RF receiver front-ends. International Computer-Aided Design Conference, pp.
302 550-553; November 1995.
- 303 2. Gomez FR, De Leon MT, Roque CR. Active balun circuits for WiMAX receiver front-end.
304 TENCON 2010 – IEEE Region 10 Conference, pp. 1156-1161; November 2010.

- 305 3. Azevedo F, Fortes F, Rosario MJ. A new on-chip CMOS active balun integrated with
306 LNA. 14th IEEE International Conference on Electronics, Circuits and Systems, pp.
307 1213–1216; December 2007.
- 308 4. Zhang HB, Cai M, Wu H, Chen HL. A 2.5GHz BiCMOS low noise and high-gain
309 differential LNA for WLAN receiver. Asia Pacific Conference on Postgraduate Research
310 in Microelectronics and Electronics, pp. 33-36; January 2009.
- 311 5. Hsu TT, Kuo CN. Low voltage 2-mW 6~10.6-GHz ultra-wideband CMOS mixer with
312 active balun. IEEE International Symposium on Circuits and Systems, pp. 5704-5707;
313 September 2006.
- 314 6. Shie CI, Hsieh CH, Chiang YC. UWB LNA and mixer with an active balun in 0.18 μ m
315 CMOS process. Asia Pacific Microwave Conference, pp. 1140-1143; December 2009.
- 316 7. Do MA, Lim WM, Ma JG, Yeo KS. Design of a phase splitter for 3rd ISM band. IEEE
317 Conference on Electron Devices and Solid-State Circuits, pp. 237-240; December 2003.
- 318 8. Kawashima M, Nakagawa T, Araki K. A novel broadband active balun. 33rd European
319 Microwave Conference, vol. 2, pp. 495-498; October 2003.
- 320 9. IEEE standard 802.16e-2005. Part 16: Air interface for fixed and mobile broadband
321 wireless access systems, Amendment 2: Physical and medium access control layers for
322 combined fixed and mobile operation in licensed bands, and Corrigendum 1. IEEE
323 Computer Society and IEEE Microwave Theory and Techniques Society; 28 February
324 2006.
- 325 10. Yang HYD, Castaneda JA. Design and analysis of on-chip symmetric parallel-plate
326 coupled-line balun for silicon RF integrated circuits. IEEE Radio Frequency Integrated
327 Circuits Symposium, pp. 527-530; June 2003.
- 328 11. Cadence Design Systems, Inc. Custom IC / analog / RF design – circuit design.
329 [https://www.cadence.com/content/cadence-www/global/en_US/home/tools/custom-ic-](https://www.cadence.com/content/cadence-www/global/en_US/home/tools/custom-ic-analog-rf-design/circuit-design.html)
330 [analog-rf-design/circuit-design.html](https://www.cadence.com/content/cadence-www/global/en_US/home/tools/custom-ic-analog-rf-design/circuit-design.html)
- 331 12. Synopsys, Inc. StarRC – parasitic extraction. [https://www.synopsys.com/](https://www.synopsys.com/implementation-and-signoff/signoff/starrc.html)
332 [implementation-and-signoff/signoff /starrc.html](https://www.synopsys.com/implementation-and-signoff/signoff/starrc.html)
333